



Fabrication of Kevlar based shielding material for attenuation of ionizing radiations

Shubham Ghag^a, Shivanand Bhushan^{a,*}, Sibi Oommen^a, Suhas Yeshwant Nayak^{b,**}, J.P. Jaideep^b, S.V. Suryanarayana^c, P.M. Prajapati^{c,d}, Sachin Shet^{c,e}, Subbaiah Kv^c, Paresh Prajapati^{c,d}

^a Department of Nuclear Medicine, Manipal College of Health Professions, Manipal Academy of Higher Education, Manipal, 576104, Karnataka, India

^b Department of Mechanical & Industrial Engineering, Manipal Institute of Technology, Manipal Academy of Higher Education, Manipal, Karnataka, 576104, India

^c Manipal Centre for Natural Sciences, Manipal Academy of Higher Education, Manipal, 576104, Karnataka, India

^d Istituto Nazionale di Fisica Nucleare, Laboratori Nazionali del Sud, Catania, 95123, Italy

^e Department of Physics, Manipal Institute of Technology, Manipal Academy of Higher Education, Manipal, Karnataka, 576104, India

ARTICLE INFO

Handling Editor: Dr. Chris Chantler

Keywords:

Radiation shielding
Composite materials
Aramid fibre
Tungsten oxide material
Bismuth oxide

ABSTRACT

The aim of this study is to fabricate a flexible, lightweight and less toxic alternative to pure lead for shielding against ionizing radiation. Composite material based on room temperature vulcanizing silicone rubber with different weight percentages of tungsten carbide, bismuth oxide and a smaller percentage of lead enrichment with Aramid fibre were fabricated. The mechanical parameters like tensile strength, percentage elongation at break, and physical property like density were measured for the prepared composites. Scanning Electron Microscope (SEM) and Energy dispersive X-ray spectroscopy (EDS) was performed for visualisation and characterization of the prepared composite. Radiation attenuation parameters like determination of Half Value Layer (HVL), Tenth Value Layer (TVL), Linear attenuation coefficient (LAC) & Mass attenuation coefficients (MAC) were carried out. Morphological and mechanical observations showed that the composition with 20% tungsten carbide: 60% Bismuth Oxide and 20% Lead showed superior mechanical properties as the concentration of Bismuth Oxide increased across the filler matrix. The sample prepared with 40 % tungsten carbide: 40% Bismuth Oxide and 20 % of Lead (TSN 3) exhibited good radiation shielding properties against the commonly used radioisotopes. Monte Carlo Neutron-Photon (MCNP) Simulation tools, are used to estimate the attenuation parameters, which are later experimentally determined using a radioactive source (Cesium-137) and Sodium Iodide detector for TSN-3 with the elemental composition.

1. Introduction

The growing applications of ionizing radiations holds great importance in medicine and technology. This increases the risk of exposure of these radiations to the occupational workers and the public (Atashi et al., 2018). The As low as reasonably achievable principle (ALARA) is one of the most crucial principles that explains the importance of factors like Time, Distance, and Shielding while dealing with ionizing radiations. Therefore, these three factors need to be maintained wherever and whenever possible. However, in some circumstances when time and distance parameters cannot be maintained, shielding holds a crucial role in minimizing the radiation exposure to a very great extent. Varieties in

a broader range of radiation-resistant materials have been developed and studied in various kinds of literature (Intom et al., 2020). Lead is the most usually involved material for protecting against ionizing radiation since it has a higher atomic number ($Z = 82$) and is modest. But, its property of easy breaking, heavyweight, and poisonousness to the human body and climate brings up an issue for the use of lead as a protected material to safeguard against ionizing radiations (Demayo et al., 1982). The use of leaded brass alloys for shielding against gamma and fast neutrons have been studied extensively (Erdem et al., 2017; Sakar et al., 2019). Another author have studied radiation shielding properties using MCNP 5 code for tellurite glasses (M.I. Sayyed et al., 2018). Use of ferroalloys have also been investigated by authors because

* Corresponding author.

** Corresponding author.

E-mail addresses: shivanand.b@manipal.edu (S. Bhushan), suhas.nayak@manipal.edu (S.Y. Nayak).

of their lower mean free path and higher mass attenuation coefficients (Büyükyıldız M et al., 2024). Several researchers have conducted studies to replace lead with an alternative material due to its toxic behaviour. Radiation shielding properties against gamma radiations using an HPGe detector and Ba-133 source was studied, where results showed excellent shielding properties when compared to glasses, concrete and other lead based shielding materials (Ersundu et al., 2018). Studies have also been conducted on Dy³⁺ doped zinc-alumino borosilicate glasses was explored for optical and gamma ray shielding features (M. Monisha et al., 2020). Varying concentrations of WO₃ with boro-tellurite glasses were synthesized and assessed for shielding against radiation, where it was observed that WO₃ concentrations improved mass attenuation coefficients and demonstrated the synthesized glass as promising material for radiation shielding (Nagaram et al., 2024). Another study demonstrated that Dy₂O₃- doped glasses exhibited superior mechanical and radiation attenuation properties (Thabit et al., 2024).

Bismuth (Bi) in Bi₂O₃ has a high atomic number (Z = 83) and high atom weight (208.98) (Chanthima et al., 2017). Because of having high Z number and non-toxic structure, bismuth is used in shielding against gamma radiations. The high Z number of Bi in Bi₂O₃ therefore increases the attenuation properties of natural rubber when incorporated in as high electromagnetic waves will be absorbed by it (Intom et al., 2020). Therefore, bismuth oxide becomes a potential substitute and has been designed for shielding against X/Gamma rays and has given promising results. Another alternative for lead can be Tungsten due to its higher atomic number and better shielding properties than pure lead (Kobayashi et al., 1997).

The current age of material science has evolved towards sustainability and that has led to the development of materials with combined properties from multiple base materials (Verma et al., 2019). Composites combine the desired properties of multiple constituent materials and allow for tailored properties in the final product. Composite materials can be classified as polymer matrix, metal matrix or ceramic matrix composites, based on the nature of the matrix material (Shehab et al., 2023). Fibre-reinforced polymer composites that are a type of polymer matrix (FRPCs) are the most widely used composites today (Iyer et al., 2023). Composite materials can be generally defined as a varied mixture of two or more different materials which results in a new property to that of its constituents and are usually evenly distributed. These constituents reinforced in the composites are generally particles, fabrics, filler materials etc (Erden and Ho, 2017). Potential applications of fibre reinforced polymers has drawn significant applications in military and electrical applications as well. The support of fiber upon polymeric network is found to achieve huge headways in mechanical ways of behaving of polymeric host with certain advantages of being light weight, increased strength to load proportion, amazing enduring secure qualities and stability of their dimensions (S et al., 2017). Fibres are the load-bearing elements in a composite and account for a significant portion of its volume. They are fixed and kept in the desired place and direction by the matrix. It also allows for easier load transfer between them while also protecting them from the elements and mechanical damage (Nayak et al., 2015). The nylon 6 based silicon rubber composites explored as an alternative for lead demonstrated promising radiation attenuation properties in a specific energy range between 140 Kev and 511 Kev with varying filler compositions of 60% Bismuth oxide and 50% Aluminium powder via hand layup technique exhibited excellent mechanical properties, including high tensile strength (25.13 MPa), elongation at break (79.3%) indicating high ductility (Govenkar PGN et al. 2024) The use of polymers has drawn a lot of attention for its applications in radiation shielding composites. Carbon fiber reinforced high performance polymers & glasses studied for mass attenuation coefficient Mean free Path like photon interactions parameters using correlation between ZXCOM, WinXCom and Monte Carlo N-Particle simulation code (MCNP) (Aral N et al., 2020; More CV et al., 2024). The use of High-performance polymers for application of radiation shielding against x-rays and gamma rays have been studied using a Ba-133

radioactive point source (M. Büyükyıldız et al., 2018)

Pure tungsten, a non-toxic element, having potential of replacing lead is very expensive (Jamal AbuAlRoos et al., 2020; Ahmed et al., 2020 studied gamma ray shielding properties of tungsten composites with room temperature vulcanization silicone rubber. Studies have been conducted on tungsten carbide as a radiation attenuation material being a cheaper alternative to Tungsten as a radiation shielding material and has shown promising results in the field of Nuclear Medicine (Jamal AbuAlRoos et al., 2020). Kevlar belongs to the polyamide group usually used for bullet-proof and fire safety wear. Its unique property of high strength, high modulus, toughness, thermal gives it a good potential for fabrication with different metal composites, which can be used as flexible, lightweight, and wearable radiation shielding material. Besides, a study has also shown good attenuation of space radiations with Kevlar compared to polyethylene that is becoming a standard for submissive shielding of radiation in space and in deep space missions to reduce harmful radiation exposure from trapped radiations (Narici et al., 2017; Gohel A & Makwana R, 2022). Kevlar has also been used as a passive radiation shielding material in space, showing varying degrees of shielding effectiveness, with dose reduction for alpha particles and protons (Al Zaman et al., 2022). Applications of silicone rubber as a polymer matrix can be done because of its inorganic nature, high flexibility, superior mechanical and physical properties as an elastomer (Yilmaz et al., 2020).

The present study aims to study the decreased concentration of lead and different fillers like bismuth oxide and tungsten carbide. Silicone rubber and Kevlar will provide flexibility, lightweight and wearable properties with reduced toxicity against the commonly used medical radioisotopes in the department of Nuclear Medicine for various diagnostic and therapeutic uses. The prepared composite material was subjected to various physical, mechanical and radiation attenuation tests. Monte-Carlo simulation was also performed to check the validation of the experimental results of radiation attenuation carried out using a radioactive gamma sources. Our study thus aims to study the radiation attenuation and mechanical property of the prepared composite material against ionizing radiations.

2. Materials & methodology

The composites were fabricated using a plain-woven aramid fabric as reinforcement, with an areal density of 200 gsm and a layer thickness of 0.25 mm. This fabric was procured from Shreeji Industries in Ahmedabad, India. Silocest Liquid Silicon Rubber was used as a matrix material with a density of 1.08 g/cc along with a compatible hardener LSR2 Fast moulding grade were obtained from Chemzest Techno Products Pvt. Ltd., Chennai, India. Three kinds of fillers were incorporated in the matrix here, which included lead and tungsten carbide that are irregular in shape along with bismuth oxide that is spherical shaped. All these three kinds of fillers were obtained from commercial suppliers. Lead metal powder was dispersed in the matrix which has an average size 40 µm having a density of 11.35 g/cc was supplied by Bhoomi Metal Alloys, Mumbai, India. Yellow coloured powder bismuth oxide having a density of 8.9 g/cc and average particle size of 10 µm, was obtained from SVG Pharma Life science Pvt. Ltd., Khopoli, India. Tungsten carbide particles, with a density of 15.63 g/cc and an average particle size of 18.5 µm was purchased from Avis Metal Industries Pvt. Ltd., Surat, India.

Hand lay-up technique was employed to fabricate the composites (Fig. 2). Each composite consisted of a single layer of 63 mm × 64 mm aramid fabric with a fiber weight fraction of 50%, embedded in a silicon rubber matrix. A consistent resin-to-hardener ratio of 50:1 was maintained for all fabricated samples. To prepare the matrix, a predetermined quantity of resin was initially poured into a mixing cup. Calculated amounts of lead, tungsten carbide and bismuth oxide as specified in Table 1, were then added and thoroughly mixed for 5 min. Subsequently, the hardener was introduced and mixed for an additional 2 min before being poured into a 1 mm thick metallic mould. An aramid fabric

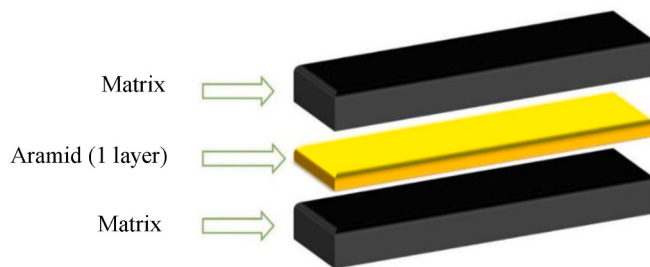


Fig. 1. Cross sectional image of composite material.

layer was later placed, followed by an additional layer of resin. The composite was then cured for 2 h at 30 °C and then ejected from the mould. The main reason of selecting this chemical composition was to examine the impact of varying levels of tungsten carbide and bismuth oxide in the composite material. This approach aimed to generate extensive data to identify the most effective composite for shielding against ionizing radiation. A cross-sectional schematic representation of the composite material is presented in Fig. 1.

2.1. Physical and mechanical properties

2.1.1. Physical properties

Density testing is crucial for composite materials as it verifies materials uniformity, detects voids or defect and ensures the material meet design specifications. Accurate density values are essential for predicting mechanical properties and optimizing composite performance across various applications. A digital density balance (Contech CAS-234) was utilized to measure the experimental density of the composite (ρ_{Ca}). Density and void content were measured on five specimens each, and the average values were calculated. The void test is performed in accordance with ASTM D2734-16, 2023. The Agarwal and Broutman equation (1) is applied to calculate the theoretical density of the laminate (ρ_{Ct}). In this context, w and ρ represent the mass fraction and density respectively, with the suffixes f , m and np indicating the fiber, matrix and nanofillers. The void fraction is then determined using equation (2).

$$\rho_{Ct} = \frac{1}{\left(\frac{w_f}{\rho_f}\right) + \left(\frac{w_m}{\rho_m}\right) + \left(\frac{w_{np1}}{\rho_{np1}}\right) + \left(\frac{w_{np2}}{\rho_{np2}}\right) + \left(\frac{w_{np3}}{\rho_{np3}}\right)} \quad (1)$$

Where.

$$\begin{aligned} w_f &= \text{weight fraction of fiber} \\ w_m &= \text{weight fraction of matrix} \\ w_{np} &= \text{weight fraction of nanoparticles} \\ \rho_f &= \text{density of fiber} \\ \rho_m &= \text{density of matrix} \\ \rho_{np} &= \text{density of nanoparticles} \end{aligned}$$

$$\text{Void fraction} = \left(\frac{\rho_{Ct} - \rho_{Ca}}{\rho_{Ct}} \right) \times 100 \quad (2)$$

Where.

$$\begin{aligned} \rho_{Ct} &= \text{theoretical density of the composite,} \\ \rho_{Ca} &= \text{actual density of the composite} \end{aligned}$$

2.1.2. Tensile strength

Tensile testing is essential for assessing a material's strength and elasticity, verifying its suitability for various applications and ensuring the safety and reliability of products. Tensile tests were conducted on Universal testing Machine (UTM) (Make: Zwick Roell Z2020) having a load cell of 20 kN. Test was conducted according to the ISO-37 standard. Five samples of each combination were subjected to tensile testing at room temperature in a UTM with a fixed crosshead speed of 500 mm/min.

2.2. Radiation parameter

A Geiger counter comprises of a Geiger-Muller tube, the detecting component which recognizes the radiation, and the handling hardware.

Table 1
Designation and composition of various components.

Sample	Weight proportion (g)		
	Lead	Tungsten Carbide	Bismuth Oxide
TSN-1	2	6	2
TSN-2	2	5	3
TSN-3	2	4	4
TSN-4	2	3	5
TSN-5	2	2	6

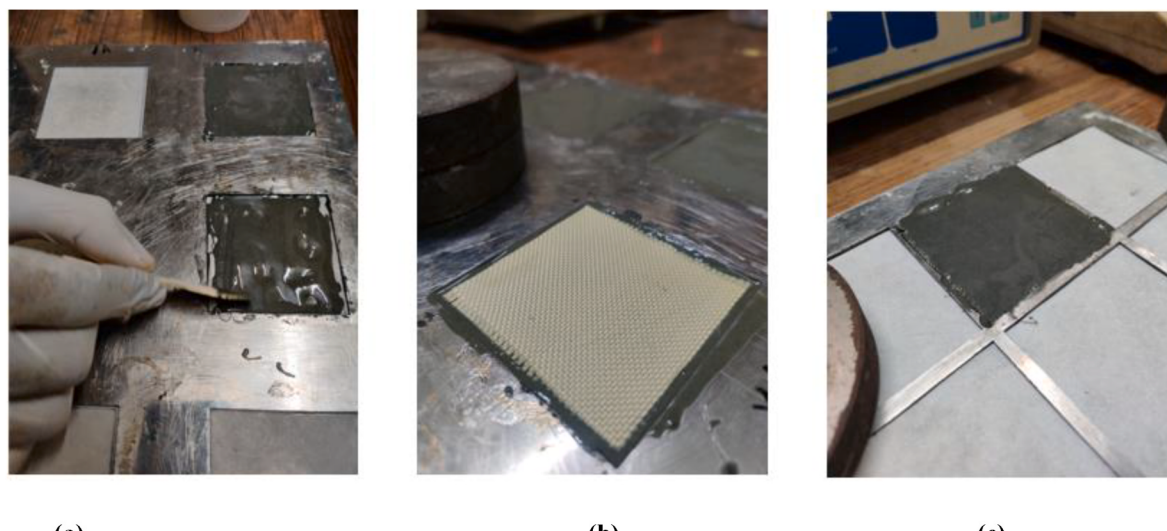


Fig. 2. Preparation of composite material using hand layup method (a) preparation of base layer matrix (b) addition of Kevlar fabric as fibre reinforcement (c) addition of top layer matrix.

Geiger-Muller tube is loaded up with an inert gas in a very low pressure applied by a high voltage. Tube momentarily directs electrical charge when a molecule or photon radiation makes the gas conductive causing ionization (Pandey et al., 2017). A Geiger Muller (GM) counter was used to check Radiation attenuation parameters for the prepared test samples as Proof of concept (PoC) & primitive prototype of novel fabricated composite materials. The quality control of GM counter was done which included various performance parameter testing like determining the operating voltage of the GM counter using a standard Cs-137 radioactive source, to assess the detector percentage efficiency of the GM counter using different sources like Cs-137 (Gamma emitter) and Sr-90 (Beta emitter) and to assess the dead time of the GM counter a point source of Tc-99 m (Gamma emitter) is used. The operating voltage was found out to be 555V. The percentage efficiency for standard Cs-137 radioactive source was found out to be 0.05% and 2.22% for Sr-90 radioactive source. After the calibration of GM counter was completed, various radiation attenuation parameters such as Half Value Layer (HVL), Tenth Value Layer (TVL), Linear attenuation coefficient (LAC) and Mass attenuation coefficient (MAC) were calculated using four different radioactive sources namely – Technetium-99 m (140 keV Gamma energy), Iodine-131 (364 keV Gamma and 606 keV beta), Fluorine-18 (511 keV annihilation photons and Lutetium-177 (497 keV beta and 208 keV gamma).

2.2.1. Half Value Layer

HVL is the thickness of a material which reduces the initial intensity of radiation to one half of its original value (Akkurt et al., 2012). The readings were taken using a GM counter where the radioisotope was placed on the 4th rack position from the detector end followed by stacking up the test samples one over the other until the initial intensity of the radiation counts was decreased to half. This value was corresponded to the thickness at that level and was considered as the HVL for that material with the respective radioisotope.

2.2.2. Tenth Value Layer

The thickness of a material in which the initial intensity is reduced by 1/10th of its original value is known as TVL of that material (Akkaş, 2016)

The value of Tenth Value Layer was obtained by the formula –

$$\text{Tenth Value Layer} = 3.32 \times \text{HVL} \quad (1)$$

2.2.3. Linear attenuation coefficient

The probability that a photon will undergo an interaction when it passes through a material is defined by linear attenuation coefficient. It has a unit of cm^{-1} (Brown et al., 2008)

LAC was obtained by using the formula –

$$\text{Linear attenuation coefficient} = \frac{0.693}{\text{Half Value Layer}} \quad (2)$$

2.2.4. Mass attenuation coefficient

Mass attenuation coefficient is a factor which is used to derive dosimetry and shielding (Vahabi et al., 2017). The MAC is the ratio of LAC divided by the density of that material.

Mass Attenuation Coefficient was calculated using the formula –

$$\text{Mass attenuation coefficient} = \frac{\text{Linear attenuation coefficient}}{\text{Density of material}} \quad (3)$$

All the fabricated test samples have been compared with lead experimental for analysing their radiation attenuation parameters. To analyse this, HVL, TVL, MAC and LAC values of the test samples were compared to lead for 4 different radioisotopes namely, Tc-99, F-18, Lu-177 & I-131. For all the isotopes, 5 values each of 4 parameters are taken for all 5 fabricated materials and lead material. Mean values of the each of the 4 parameters of all 5 fabricated material are compared with lead

in following ways: Normality and homogeneity of variance assumptions are verified by applying Shapiro Wilk test and F test respectively. For all the isotopes, Mean HVL value of TSN-1, TSN-2, TSN-3, TSN-4 and TSN-5 are all compared with Mean HVL value of lead by performing independent sample *t*-test for each. Similar analysis is carried out for other 3 parameters.

3. Results and discussion

3.1. Physical properties

Table 2 presents the densities and void fraction of the composites. Change in the actual densities of the composites with respect to theoretical densities can be observed, which is attributed to the presence of voids or air gaps. These defects cause a reduction in the actual density compared to the theoretical density. As indicated in **Table 2**, the composite material's density diminishes from TSN-1 to TSN-5. This is attributed to the decreasing proportion of tungsten carbide particles within the composite, given the higher density of tungsten carbide, its reduced content contributes to an overall decrease in the theoretical density of the composite. The presence of bismuth oxide, which has a lower density, also contributes to the decrease in density. TSN-1, TSN-2 and TSN-3 exhibited lower void fractions compared to the other two test samples, indicating reduced void content in these composites. Overall, the void content in all the composites is within acceptable limits and did not adversely affect their properties.

3.2. Mechanical properties

Tensile test revealed that TSN-1 exhibited the lowest tensile strength of 5.34 MPa. This sample contained the highest concentration of tungsten carbide, characterized by irregularly shaped particles that promoted crack initiation and propagation. The complex interface between tungsten carbide and the matrix hindered strong bonding. Gradual increase in tensile strength could be noted in TSN-2 and TSN-3 with 6.76 MPa and 6.98 MPa respectively. TSN-4 exhibited a tensile strength of 7.44 MPa. TSN-5 demonstrated the highest tensile strength of 8.46 MPa and 58.42% improvement in tensile strength can be observed in comparison with TSN-1. The uniform dispersion of spherical bismuth oxide particles in the matrix efficiently transferred load and acted as stress concentrators, enhancing the material's ability to bear tensile loads. It can be inferred that addition of bismuth oxide results in increase in tensile strength. A graphical representation of these results can be found in **Fig. 3**.

Similar trend was followed by sample tested for elongation at break. The recorded elongation at break for the test samples showed that TSN-1 had an elongation of 52.46% and TSN-2 had an elongation of 58.42%. As the bismuth oxide content increased and the tungsten carbide content decreased, there was an improvement in elongation at break. This increasing trend continued with TSN-3, TSN-4, and TSN-5, which exhibited elongations of 65.32%, 72.6%, and 78.9% respectively. All test samples demonstrated adequate tensile strength and elongation at break, making them suitable for use in radiation shielding apron applications.

Table 2
Density and void fraction.

Test Sample	Theoretical Density (g/cc)	Actual Density (g/cc)	Void Fraction (%)
TSN-1	1.6713	1.6403	1.8548
TSN-2	1.6679	1.6329	2.0984
TSN-3	1.6646	1.6304	2.0545
TSN-4	1.6612	1.6228	2.3115
TSN-5	1.6579	1.6199	2.2920

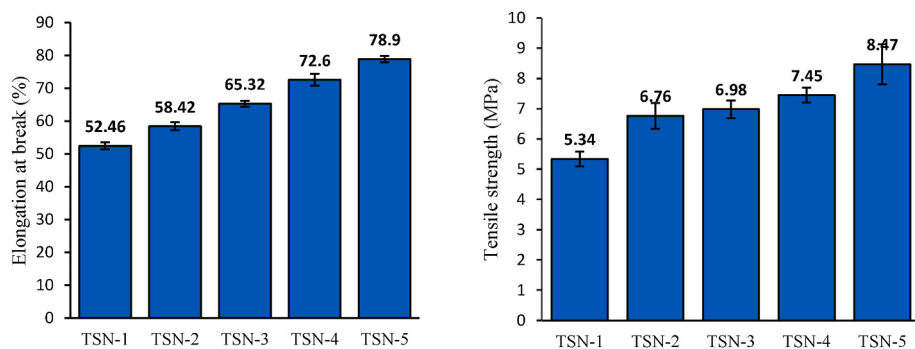


Fig. 3. Tensile strength and % Elongation at break.

3.3. Scanning electron microscope

SEM micrographs of all the fabricated composites are shown in Fig. 4. In Fig. 4a bismuth oxide can be seen in a few places and appears like tiny spherical structures. The major filler content in TSN-1 is 60% of tungsten carbide and is seen irregular in shape and uniformly distributed throughout the matrix. Few chunks of lead particles are also present in the matrix. Fig. 4b represents TSN-2 wherein tungsten carbide particles are equally spread across the matrix. A small crater is formed due to displacing of fillers. Irregular shaped Lead particle could be observed in

the image. In addition to this a cluster formation is seen which has different particles in it. The surface morphology of TSN-3 is shown in Fig. 4c which has various size of Bi_2O_3 particles. Chunks of Tungsten Carbide and Lead particles can be noted. No voids or cluster formation could be seen in the matrix. The dispersion of filler seems to be uniform throughout the surface. SEM micrograph of TSN-4 is portrayed in Fig. 4d which comprises of 20% lead, 30% tungsten carbide and 50% bismuth oxide. Pocket formation could be seen in few places due to displacing of filler from its place. Bismuth oxide particles are spread across the matrix. Bits of tungsten carbide and lead fillers are well scattered. Overall

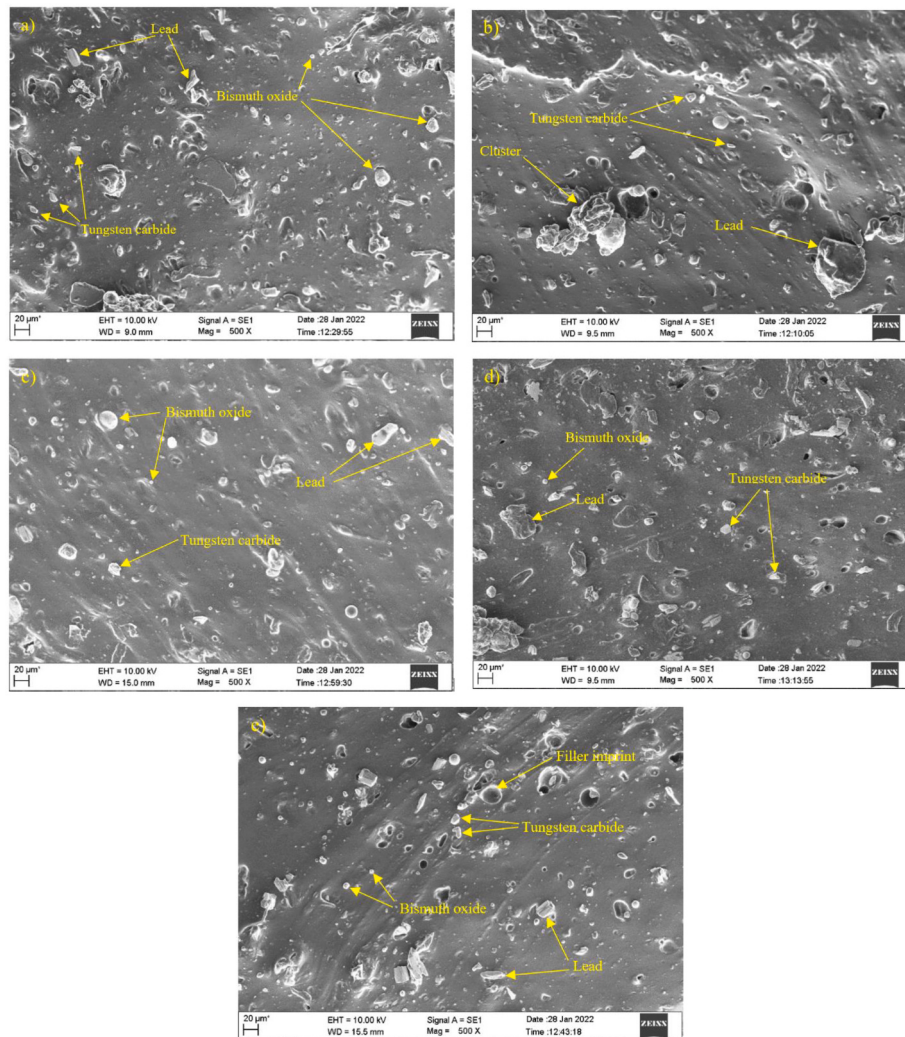


Fig. 4. SEM micrographs of a) TSN-1 b) TSN-2 c) TSN-3 d) TSN-4 e) TSN-5.

dispersion of filler in matrix seems uniform. Bismuth oxide is evenly distributed all over the matrix surface in TSN-5 Fig. 4e. Fillers that came apart from the matrix leaving behind its imprint is seen in the top of the image. This is caused while preparing sample for SEM. Uniform distribution of tungsten carbide and few pieces of lead is detected. Overall the distribution of particles seemed to be better than other test samples with no evidence agglomeration was found.

3.4. Radiation attenuation parameters of the composites

To investigate the radiation attenuation parameters of the prepared composite samples; Tc-99 m, I-131, F-18 and Lu-177 radioisotopes were used. This test was done using a GM counter. Various parameters like HVL, TVL, LAC and MAC were calculated for all the composite samples. As the energy of the radioisotope increased, the value of HVL and TVL also increased, resulting in decreased attenuation on photons radiating out of the source. Lesser the value of HVL, better is the material for attenuating the radiation emitted. Fig. 5 shows a combined graphical representation of HVL and TVL of all samples compared with lead standard.

3.5. Simulations of TSN-3 attenuations

As Aluminium is also a good attenuator for the low energy nuclear radiations the present new composite properties such as Mass attenuation co-efficient (MAC) has been compared with the Monte-Carlo simulation tools (Battistoni et al., 2015). From Fig. 6 it is clear that the estimated MACs for the new composite are better than aluminium at lower energies. Further the new composite has been experimentally tested using radioactive sources to validate the simulation carried out. The gamma lines 59 keV (Am-241), 511 keV (Na-22), and 662 keV (Cs-137) have been used, the attenuation by the composite is measured with the Sodium Iodide detector setup. Source activity of Am-241: 3.64 kBq Na-22: 28.70 kBq & Cs-137: 285.96 kBq. Source activity calculated on the date of the experiment carried out. The detector efficiency at 5 cm from the source at 662 keV is nearly 3.1%. Broad beam geometry used in the work, where the sample kept at 5 mm from the detector, with source to detector distance of 5 cm. From the figure it is clear that the experimental data are in good agreement with the simulation carried out. The new composite found to be good at lower energies despite being less

Comparison of Mass Attenuation co-efficient

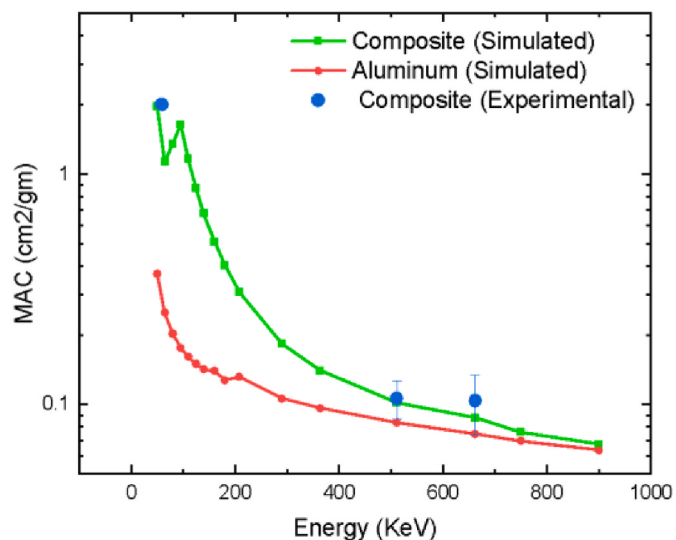


Fig. 6. Mass attenuation co-efficient for aluminium vs simulated & experimental composite material.

dense compared to Aluminium.

In this study, the mass attenuation coefficient of the prepared composite material was investigated using established gamma lines at 59 keV (Am-241), 511 keV (Na-22), and 662 keV (Cs-137), and compared against the performance of lead. The mass attenuation co-efficient at 662 keV is found to be 0.08742 cm²/gm. Linear attenuation coefficient is 0.14252 cm⁻¹. Mean free path lambda = 1/LAC = 7.04 cm. MFP lead 0.8 cm. As illustrated in Fig. 7, the mass attenuation values for both the composite and lead decrease with increasing energy. While lead demonstrates higher mass attenuation coefficient values across the energy range, indicating superior attenuation performance in this direct comparison, the composite material still exhibits significant attenuation capabilities. This suggests the composite effectively interacts with incident radiation but to a lesser degree than lead. While the fabricated composite did not outperform lead, it demonstrated promising attenuation characteristics with good mechanical properties. Further research

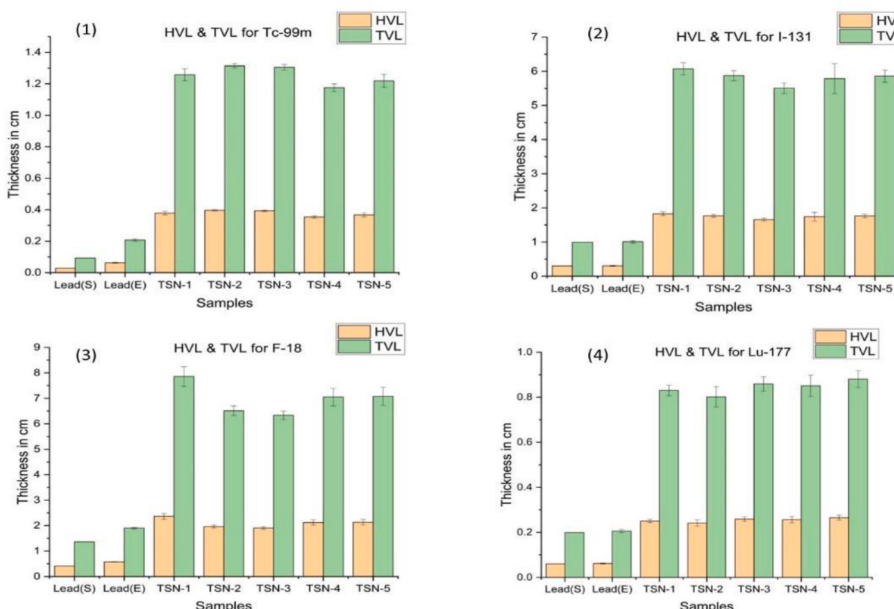


Fig. 5. Graph of Mean ± SD values for HVL and TVL for all samples with lead standard and lead experimental.

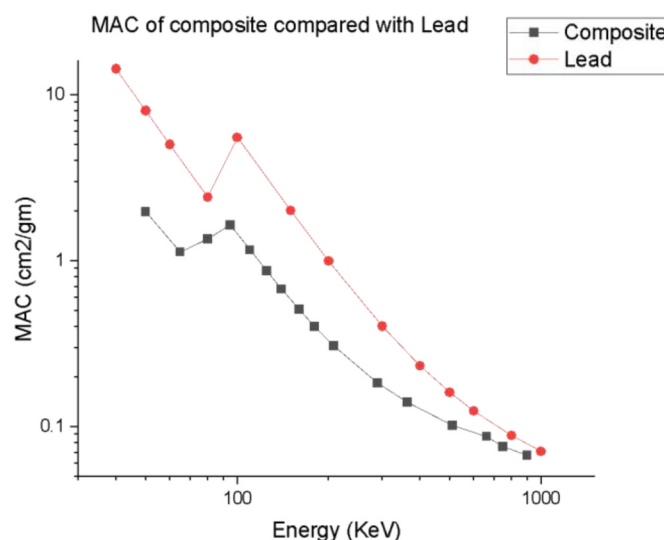


Fig. 7. Mass attenuation co-efficient for lead vs simulated composite material.

could explore avenues to enhance the composites shielding properties, potentially through compositional modifications or structural optimizations. Moreover, the composite may offer advantages in aspects such as cost-effectiveness, ease of handling or specific application requirements where weight or flexibility are paramount.

When the prepared composites were checked for determining the tensile strength, it was found that TSN-5 showed the highest value of tensile strength as 8.46 MPa. The increase in tensile strength as the concentration of bismuth oxide increases across the filler matrix could be due to less agglomerations of bismuth oxide particles due to its structure and tungsten carbide exhibiting more agglomerations. This was due to the particles being uniformly dispersed and fewer cluster formations of tungsten carbide particles. Therefore, there was a good bond of the fabric with matrix with samples containing lesser concentration of tungsten carbide particles.

Assessment of radiation attenuation parameters for all the fabricated test samples was conducted. Measurement of this was done with different energy levels of radioisotope from 140 keV to 511 keV including beta, positron, and gamma radiations. It was noted that the values of all 5 composite materials differed significantly from radiation attenuation parameters of lead when the p value was kept 0.5. It was concluded that there was no significant difference in the radiation attenuation parameters of all the 5 fabricated samples when compared intergroup. This could either be possible because of the formation of voids and agglomerations of tungsten carbide particles in all the samples as a result of using the hand-mixing methods as confirmed from the SEM-EDS analysis. It is very important while fabricating such composites that there should be minimal or no agglomeration of particles for best and uniform results. [Intom et al. \(2020\)](#) and [Kalkornsurapranee et al. \(2021\)](#) obtained an HVL of approximately 3.6 cm and 3.8 cm at 663 keV energy. The author fabricated the composite materials using an Internal mixer. Considering the test samples fabricated in this study TSN-4 gave an HVL of 0.35 cm at 140 keV for Tc-99 m radioisotope. Therefore, the prepared composite samples in this study can possibly show close or better results to the prepared composites. [Noor Azman et al., 2013](#) in their study have experimented with different filler loading wt% of PbCl₂, Bi₂O₃ and WO₃ for attenuation of x-rays. [Chang et al., 2015](#) in their work have studied increasing concentration of tungsten with silicone rubber based matrix. Therefore, future studies can be conducted by incorporating more filler composition by increasing the ratio and testing their mechanical and radiation attenuation properties. Although TSN-5 Bi60:W20 showed superior mechanical properties than all other test samples, BI40:W40 TSN-3 showed better radiation

shielding properties. [Govenkar et al. \(2024\)](#) successfully fabricated nylon-6 based composite material which demonstrated radiation shielding properties. Their study revealed HVL of 2.06 cm for energy range from 140 keV–511 keV. When compared to the fabricated Kevlar based composite material, our study showed superior radiation shielding characteristics for TSN-3 with an HVL of 0.39 cm, 1.65 cm, 1.90 cm & 0.25 cm for Tc-99 m, I-131, F-18 & Lu-177 radioisotopes respectively. The following HVL values when compared with the prepared silicone rubber composites in this study demonstrates that TSN-3 composite have demonstrated a great potential to be used as a flexible, lightweight shielding material. Lack of studies conducted on positron and beta emitting radiation sources gives potentiality to this study in terms of shielding aspects for commonly used radioisotopes in the department of Nuclear Medicine. While our study provides valuable insights into the radiation attenuation and mechanical properties of the developed composite material, it is important to note that compliance with the EN/IEC 61331-1:2014 standards was not considered, as this study focused on initial conceptual design for novel composite fabrication phase of Technology Readiness Level (TRL-1) and early prototype stage (TRL 2/3/4). Further studies will aim to incorporate the EN/IEC 61331-1:2014 standard compliance more rigorously, ensuring that materials undergo standardized testing for radiation shielding effectiveness measurements ([Demirel I & Yucel H, 2024](#)), thus enhancing reliability and applicability of results before Go to Market (GTM)/Pre commercial deployment (TRL-5 onwards) of product compliance standard.

4. Conclusion

Silicone rubber-based aramid composites with varying bismuth oxide, tungsten carbide, and lead content were synthesized and characterized for mechanical and radiation attenuation properties. TSN-3 exhibited the highest radiation shielding performance, particularly against low-energy X-rays, corroborated by Monte Carlo simulations. While not surpassing lead's attenuation, TSN-3 demonstrated promising combined radiation shielding and mechanical properties, suggesting its potential as a flexible, lightweight, and less toxic alternative for ionizing radiation shielding and warranting further optimization studies as per EN/IEC 61331-1:2014 product compliance standard.

CRediT authorship contribution statement

Shubham Ghag: Writing – original draft, Formal analysis, Data curation. **Shivanand Bhushan:** Writing – review & editing, Writing – original draft, Supervision. **Sibi Oommen:** Supervision, Writing – original draft, Writing – review & editing. **Suhas Yeshwant Nayak:** Writing – original draft, Data curation. **J.P. Jaideep:** Writing – review & editing, Supervision, Project administration, Data curation, Conceptualization. **S.V. Suryanarayana:** Writing – review & editing, Writing – original draft, Supervision. **P.M. Prajapati:** Writing – original draft, Methodology, Investigation, Formal analysis, Data curation. **Sachin Shet:** Writing – review & editing, Supervision. **Subbaiah Kv:** Writing – review & editing, Supervision. **Paresh Prajapati:** Writing – review & editing, Writing – original draft, Supervision.

Data availability

No data was used.

Funding sources

NIL This research did not receive any specific grant from funding agencies in the public, commercial, or not-for-profit sectors.

Declaration of competing interest

The authors declare that they have no known competing financial interests or personal relationships that could have appeared to influence the work reported in this paper.

Acknowledgement

Authors are thankful to Dean MCHP Manipal, Director MIT Manipal & Director MCNS Manipal for providing the support to complete the work. Expressing gratitude to MAHE FAIMER & associated mentors for ideation & conceptualisation of new materials composites for developing need-based radiation emergency tools & devices. Expressing thanks to DOR MAHE Manipal & Dr Varadharajan S of IPTTO MAHE for facilitating Patent filing.

Data availability

Data will be made available on request.

References

- Ahmed, B., Shah, G.B., Malik, A.H., Aurangzeb, Rizwan, M., 2020. Gamma-ray shielding of flexible silicone tungsten composites. *Appl. Radiat. Isot.* 155, 108901. <https://doi.org/10.1016/j.apradiso.2019.108901>.
- Akkaş, A., 2016. Determination of the tenth and half value layer thickness of concretes with different densities. *Acta Phys. Pol. A* 129 (4), 770–772. <https://doi.org/10.12693/APhysPolA.129.770>.
- Akkurt, I., Altindag, R., Gunoglu, K., Sarikaya, H., 2012. Photon attenuation coefficients of concrete including marble aggregates. *Ann. Nucl. Energy* 43, 56–60. <https://doi.org/10.1016/j.anucene.2011.12.031>.
- Al Zaman, M.A., Islam, M.R., Maruf, H.M.A.R., Nizam, Q.M.R., 2022. Effectiveness of Kevlar and water-soaked hygienic wipes in a combined radiation shield for manned long termed space missions. *Radiat. Phys. Chem.* 201, 110483. <https://doi.org/10.1016/j.radphyschem.2022.110483>.
- Aral, N., Duch, M.A., Ardanuy, M., 2020. Material characterization and Monte Carlo simulation of lead and non-lead X-Ray shielding materials. *Radiat. Phys. Chem.* 174, 108892. <https://doi.org/10.1016/j.radphyschem.2020.108892>.
- ASTM D2734-16, 2023. Standard test methods for void content of reinforced plastics. <http://www.astm.org/d2734-16.html>.
- Atashi, P., Rahmani, S., Ahadi, B., Rahmati, A., 2018. Efficient, flexible and lead-free composite based on room temperature vulcanizing silicone rubber/W/Bi2O3 for gamma ray shielding application. *J. Mater. Sci. Mater. Electron.* 29 (14), 12306–12322. <https://doi.org/10.1007/s10854-018-9344-1>.
- Battistoni, G., Boehlen, T., Cerutti, F., Chin, P.W., Esposito, L.S., Fasso, A., Ferrari, A., Lechner, A., Empl, A., Mairani, A., Mereghetti, A., 2015. Overview of the FLUKA code. *Ann. Nucl. Energy* 82, 10–18. <https://doi.org/10.1016/j.anucene.2014.11.007>.
- Brown, S., Bailey, D.L., Willowson, K., Baldock, C., 2008. Investigation of the relationship between linear attenuation coefficients and CT Hounsfield units using radionuclides for SPECT. *Appl. Radiat. Isot.* 66 (9), 1206–1212. <https://doi.org/10.1016/j.apradiso.2008.01.002>.
- Büyükyıldız, M., Taşdelen, M.A., Karabul, Y., Çağlar, M., İçelli, O., Boydacı, E., 2018. Measurement of photon interaction parameters of high-performance polymers and their composites. *Radiat. Eff. Defect Solid* 173 (5–6), 474–488. <https://doi.org/10.1080/10420150.2018.1477155>.
- Büyükyıldız, M., Thakur, S., Levet, A., Kaur, P., 2024. Gamma-ray attenuation properties of some heavy metal ferroalloys for potential applications. *Prog. Nucl. Energy* 176, 105382. <https://doi.org/10.1016/j.pnucene.2024.105382>.
- Chang, L., Zhang, Y., Liu, Y., Fang, J., Luan, W., Yang, X., Zhang, W., 2015. Preparation and characterization of tungsten/epoxy composites for γ -rays radiation shielding. *Nucl. Instrum. Methods Phys. Res. Sect. B Beam Interact. Mater. Atoms* 356–357, 88–93. <https://doi.org/10.1016/j.nimb.2015.04.062>.
- Chanthima, N., Kaewkhaos, J., Limkitjaroenporn, P., Tuscharoen, S., Kothan, S., Tungjai, M., Kaewjaeng, S., Sarachai, S., Limsuwan, P., 2017. Development of BaO-ZnO-Bi2O3 glasses as a radiation shielding material. *Radiat. Phys. Chem.* 137, 72–77. <https://doi.org/10.1016/j.radphyschem.2016.03.015>.
- Demayo, A., Taylor, M.C., Taylor, K.W., Hodson, P.V., Hammond, P.B., 1982. Toxic effects of lead and lead compounds on human health, aquatic life, wildlife plants, and livestock. *CRC Crit. Rev. Environ. Control* 12 (4), 257–305. <https://doi.org/10.1080/10643388209381698>.
- Demirel, İ., Yücel, H., 2024. Development of a flexible composite based on vulcanized silicon casting with bismuth oxide and characterization of its radiation shielding effectiveness in diagnostic X-ray energy range and medium gamma-ray energies. *Nucl. Eng. Technol.* <https://doi.org/10.1016/j.net.2024.02.016>.
- Erden, S., Ho, K., 2017. 3—fiber reinforced composites. In: Seydibeyoğlu, M.Ö., Mohanty, A.K., Misra, M. (Eds.), *Fiber Technology for Fiber-Reinforced Composites*. Woodhead Publishing, pp. 51–79. <https://doi.org/10.1016/B978-0-08-101871-2.00003-5>.
- Ersundu, A.E., Büyükyıldız, M., Ersundu, M.Ç., Şakar, E., Kurudirek, M.J.P.N.E., 2018. The heavy metal oxide glasses within the WO₃-MoO₃-TeO₂ system to investigate the shielding properties of radiation applications. *Prog. Nucl. Energy* 104, 280–287. <https://doi.org/10.1016/j.pnucene.2017.10.008>.
- Gohel, A., Makwana, R., 2022. Multi-layered shielding materials for high energy space radiation. *Radiat. Phys. Chem.* 197, 110131. <https://doi.org/10.1016/j.radphyschem.2022.110131>.
- Govenkar, P.G., Nayak, S.Y., Oomen, S., Bhushan, S., 2024. Fabrication, characterization and investigation of flexible light weight nylon-6 based silicon rubber composites for radiation attenuation. *Radiat. Phys. Chem.* 220, 111676. <https://doi.org/10.1016/j.radphyschem.2024.111676>.
- Intom, S., Kalkornsurapranee, E., Johns, J., Kaewjaeng, S., Kothan, S., Hongtong, W., Chaiphaksa, W., Kaewkhaos, J., 2020. Mechanical and Radiation Shielding Properties of Flexible Material Based on Natural Rubber/.
- Iyer, T., Nayak, S.Y., Hiremath, A., Heckadka, S.S., Jaideep, J.P., 2023. Influence of TiO₂ nanoparticle modification on the mechanical properties of basalt-reinforced epoxy composites. *Cogent Engineering* 10 (1), 2227397. <https://doi.org/10.1080/23311916.2023.2227397>.
- Jamal AbuAlRoos, N., Azman, M.N., Baharul Amin, N.A., Zainon, R., 2020. Tungsten-based material as promising new lead-free gamma radiation shielding material in nuclear medicine. *Phys. Med.* 78, 48–57. <https://doi.org/10.1016/j.ejmp.2020.08.017>.
- Kalkornsurapranee, E., Kothan, S., Intom, S., Johns, J., Kaewjaeng, S., Kedkaew, C., Chaiphaksa, W., Sareein, T., Kaewkhaos, J., 2021. Wearable and flexible radiation shielding natural rubber composites: effect of different radiation shielding fillers. *Radiat. Phys. Chem.* 179, 109261. <https://doi.org/10.1016/j.radphyschem.2020.109261>.
- Kobayashi, S., Hosoda, N., Takashima, R., 1997. Tungsten alloys as radiation protection materials. *Nucl. Instrum. Methods Phys. Res. Sect. A Accel. Spectrom. Detect. Assoc. Equip.* 390 (3), 426–430. [https://doi.org/10.1016/S0168-9002\(97\)00392-6](https://doi.org/10.1016/S0168-9002(97)00392-6).
- Monisha, M., D'souza, A.N., Hegde, V., Prabhu, N.S., Sayyed, M.I., Lakshminarayana, G., Kamath, S.D., 2020. Dy3+ doped SiO₂-B₂O₃-Al₂O₃-NaF-ZnF₂ glasses: an exploration of optical and gamma radiation shielding features. *Curr. Appl. Phys.* 20 (11), 1207–1216. <https://doi.org/10.1016/j.cap.2020.08.004>.
- More, C.V., Tarwal, N.L., Botewad, S.N., Anis, M., Kutwade, V.V., Akman, F., Agar, O., Pawar, P.P., 2024. Radiation shielding efficacy of unsaturated polyester composites for gamma and neutron attenuation-enhanced with SnO₂. *Radiat. Phys. Chem.* 19, 112484. <https://doi.org/10.1016/j.radphyschem.2024.112484>.
- Nagaram, S.M., Hashim, S., Sanusi, M.S.M., Ibrahim, A., 2024. Enhanced physical, optical and radiation shielding properties of tungsten modified potassium borotellurite glass systems: theoretical approach. *Radiat. Phys. Chem.* 112355. <https://doi.org/10.1016/j.radphyschem.2024.112355>.
- Narici, L., Casolino, M., Di Fino, L., Larosa, M., Picozza, P., Rizzo, A., Zacone, V., 2017. Performances of Kevlar and Polyethylene as radiation shielding on-board the International Space Station in high latitude radiation environment. *Sci. Rep.* 7 (1), 1644. <https://doi.org/10.1038/s41598-017-01707-2>.
- Nayak, S., Heckadka, S., Rao, S., Narang, K., Kirti, V., Pant, 2015. Mechanical properties of multi layer plain weave and 3-D glass fabric epoxy composites. *Int. J. Compos. Mater.* 2015, 30–36. <https://doi.org/10.5923/j.cmaterials.20150502.02>.
- Noor Azman, N.Z., Siddiqui, S.A., Low, I.M., 2013. Synthesis and characterization of epoxy composites filled with Pb, Bi or W compound for shielding of diagnostic x-rays. *Appl. Phys. A* 110 (1), 137–144. <https://doi.org/10.1007/s00339-012-7464-7>.
- Pandey, S., Pandey, A., Deshmukh, M., Shrivastava, A., 2017. Role of Geiger Muller Counter in Modern Physics, pp. 192–196.
- S, P., Km, S., K, N., S, S., 2017. Fiber reinforced composites—a review. *J. Mater. Sci. Eng.* 6 (3). <https://doi.org/10.4172/2169-0022.1000341>.
- Şakar, E., Büyükyıldız, M., Alim, B., Şakar, B.C., Kurudirek, M., 2019. Leaded brass alloys for gamma-ray shielding applications. *Radiat. Phys. Chem.* 159, 64–69. <https://doi.org/10.1016/j.radphyschem.2019.02.042>.
- Sayyed, M.I., Issa, S.A., Büyükyıldız, M., Dong, M., 2018. Determination of nuclear radiation shielding properties of some tellurite glasses using MCNP5 code. *Radiat. Phys. Chem.* 150, 1–8. <https://doi.org/10.1016/j.radphyschem.2018.04.014>.
- Shehab, E., Meirbekov, A., Amantayeva, A., Tokbotal, S., 2023. Cost modelling for recycling fiber-reinforced composites: state-of-the-art and future research. *Polymers* 15 (1). <https://doi.org/10.3390/polym15010150>. Article 1.
- Thabit, H.A., Alajerami, Y.S.M., Mhareb, M.H.A., Hashim, S., Mitwalli, M., 2024. Thermal, and radiation shielding properties of Sr-O-B₂O₃-TeO₂-ZnO-Bi₂O₃ glasses doped with Dy₂O₃. *Ceram. Int.* <https://doi.org/10.1016/j.ceramint.2024.05.273>.
- Vahabi, S.M., Bahreinpour, M., Zafarghandi, M.S., 2017. Determining the mass attenuation coefficients for some polymers using MCNP code: a comparison study. *Vacuum* 136, 736. <https://doi.org/10.1016/j.vacuum.2016.11.011>.
- Verma, A., Negi, P., Singh, V.K., 2019. Experimental analysis on carbon residuum transformed epoxy resin: chicken feather fiber hybrid composite. *Polym. Compos.* 40 (7), 2690–2699. <https://doi.org/10.1002/pc.25067>.
- Yilmaz, S.N., Güngör, A., Özdemir, T., 2020. The investigations of mechanical, thermal and rheological properties of polydimethylsiloxane/bismuth (III) oxide composite for X/Gamma ray shielding. *Radiat. Phys. Chem.* 170, 108649. <https://doi.org/10.1016/j.radphyschem.2019.108649>.